

Study on Applicability of Melling Equation and Conventional Equation for Sound Absorption Coefficient Prediction of Perforated Panel at Low Sound Pressure Field

Masaaki Mori¹, Takayuki Masumoto², Kunihiko Ishihara³
^{1,2}Cybernet Systems CO., LTD

³Department of Health and Welfare, Tokushima Bunri University

(¹m-mori@cybernet.co.jp, ²masumoto@cybernet.co.jp, ³k-ishihara@fe.bunri-u.ac.jp)

Abstract- In this paper, we compared sound absorption coefficients of several perforated panels experimentally and analytically derived. The first objective of this study is to confirm the applicability both of the Melling equation and conventional equation those are used in order to calculate the acoustic behaviors in perforated panels. Although the Melling equation is regarded available under high sound pressure fields (such as over 130 dB), one of the objectives of this study is to confirm the validity of the Melling equation under the low sound pressure level (below 100 dB). Therefore, the study was performed under the low sound pressure environment. And another objective is to confirm the relationship between orifice parameters (such as orifice diameter, length and aperture ratio) and characteristics of sound absorption coefficients curve in frequency domain. In this study, the aperture ratio, orifice length and orifice diameter of the perforated plate range from 0.5 % to 8 %, from 1.0 mm to 4.6 mm and from 1.0 mm to 3.0 mm, respectively. And to investigate the effect of the structural vibration of the duct on the sound absorption coefficients of the perforated plate, we made the duct with acrylic plates. The changes of the peak value, peak frequency and half-value width of the absorption coefficients against parameter shifts derived from experimental model show almost the same trend to those of analytical model except in existence of small difference at the peak value of sound absorption coefficient. In this study, the result calculated by using the Melling equation is closer to the experimental value than the result calculated by using the conventional equation. It seems that these equations are applicable to model the acoustic behavior of the perforated panel under the low pressure environment. In addition, it was clarified that the absorption coefficients of the perforated plates are affected by the structure vibration of the duct.

Keywords- *Self-Sustained Tone, Acoustic Resonance, Lock-in Phenomenon, Perforated Plate, CFD and BEM*

I. INTRODUCTION

The number of cases where high level noise is generated due to the high performance of industrial machines is

increasing. On the other hand, noise reduction is required more than ever due to the strengthening of environmental regulations. Although high performance and low noise are in a conflicting relationship, if both are not realized, for example, operations will be stopped in the case of factories, and market competitiveness will be reduced in the case of industrial products. For this reason, noise suppression is an important issue comparable to improving product performance. Sound absorbing materials are often used as an important means for suppressing noise. Porous materials such as glass wool and urethane foam are often used as sound absorbing materials, and there are many researches on sound absorbing properties of these materials. However, these are assumed to be used in a stationary medium at room temperature, and they are difficult to use because they have a problem of durability when it is used at high temperatures and under high-speed flow. The perforated plate is known to have a sound-absorbing effect even when it is used alone. Since it can enhance the sound-absorbing effect when it is used with a sound-absorbing material such as glass wool, it is often used as a sound-absorbing panel in combination with a sound-absorbing material [1-2]. However, when it is used with a sound absorbing material, the durability problem still occurs. On the other hand, depending on the installation situation, there are cases where a perforated plate alone can provide a sufficient sound absorption effect. For example, when it is installed inside a heat exchanger duct or the inner surface of an aircraft engine nacelle, it is exposed to a high-temperature, high-speed medium, however there have been reports of successful examples of suppressing noise using only a porous plate without using a porous material [3]. There is a detailed study by Melling [4] on the sound absorbing effect of a perforated plate alone under high sound pressure level above 135 dB. Furthermore, Utsuno et al. [5] compared the measured and predicted sound absorption coefficient obtained from Melling equation under normal sound pressure for a porous plate with an orifice diameter of 2 mm, plate thickness of 0.8 mm, and aperture ratio of 2%. It is confirmed that Melling equation can be applied even under normal sound pressure, and that the amplitude dependence disappears below 80 dB [5].

In this paper, the scope of the study was expanded to several types of perforated plates (opening ratio: 8% or less, orifice length: 1.0 mm to 4.6 mm, orifice diameter: 1.0 mm to 3.0 mm), and the applicability of Melling equation under normal sound pressure was confirmed. For modeling the sound absorption effect of the perforated plate, a model that takes into account the acoustic energy loss due to the viscosity and heat exchange in the inner wall of the orifice in a resonant system with the air inside the orifice as mass and the back air layer as a spring (hereafter: simple model), has been often used in the past [6]. Therefore, we compared the simple model with Melling equation and confirmed their applicability. Furthermore, the relationship between these parameters and the sound absorption coefficient were clarified by parameter study using changes of the aperture ratio, orifice length, and orifice diameter. In addition, the effect of the structural mode of the tube on the sound absorption coefficient was also examined. Normally, when measuring the sound absorption coefficient of a perforated plate or a sound absorbing material, an acoustic tube that is assumed to be a rigid body is used. However, in many cases, the tube may not be actually considered as a rigid body. Therefore, the influence of the structural mode of the tube on the sound absorption rate was also investigated.

II. EXPERIMENT

A. Analysis Model

Figure 1 shows the model considered in this study. A perforated plate with a cylindrical orifice is sandwiched between two rectangular sound fields, and a sound field that is assumed to be one-dimensional on an axis perpendicular to the perforated plate is used. A speaker was used as a sound source. For convenience, the sound field was divided into three parts. The acoustic space excited by the speaker is Field 1, the cylindrical space inside the perforated plate is Field 2, and the space on the opposite side of the perforated plate from the sound source is Field 3. Figure 2 shows the one of the orifices. As shown in Fig. 2, the partial model of Field 1, Field 2 and Field 3 was considered, and a one-dimensional property of the acoustic field is assumed.

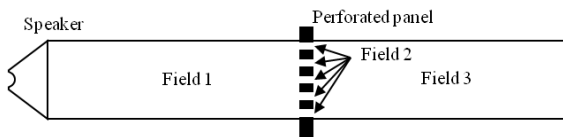


Figure 1. Analysis Model.

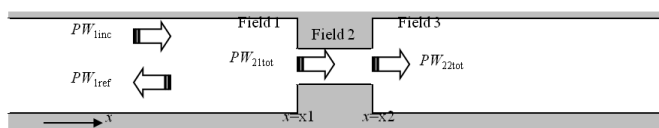


Figure 2. Values used in this study.

The general solution of the wave equation in each space is as follows.

$$p_n = j\omega\rho_n(A_n \exp[-jk_n x] + B_n \exp[jk_n x]) \quad (1)$$

$$v_n = jk_n(A_n \exp[-jk_n x] - B_n \exp[jk_n x]) \quad (2)$$

Where n : integer from 1 to 3 corresponding to Field 1 to Field 3, p : sound pressure, v : acoustic particle velocity, j : imaginary unit, ω : angular velocity, ρ : medium density, k : wave number, x : coordinate, A and B are variables.

In Field 1, we considered PW_{1inc} and PW_{1ref} as the acoustic power (W/m²) of incident and reflected waves, respectively. PW_{21tot} is considered as the acoustic power flowing into Field 2 at the entrance of Field 2, and PW_{22tot} is considered as the acoustic power flowing out at the exit of Field 2. Each sound power is expressed as follows using A , B , p , v in Eqs. (1) and (2).

$$PW_{1inc} = 0.5 \frac{\omega^2 \rho_1}{c_1} |A_1|^2 S_1 \quad (3)$$

$$PW_{1ref} = -0.5 \frac{\omega^2 \rho_1}{c_1} |B_1|^2 S_1 \quad (4)$$

$$PW_{21tot} = -0.5 S_2 p_2|_{x=x_1} (v_2|_{x=x_1})^* \quad (5)$$

$$PW_{22tot} = -0.5 S_2 p_2|_{x=x_2} (v_2|_{x=x_2})^* \quad (6)$$

Here c is the speed of sound, S is the effective area, $p_n|_{x=x_0}$ is the sound pressure at $x = x_0$ of Field n , $v_n|_{x=x_0}$ is the acoustic particle velocity at $x = x_0$ of Field n . $|A_1|$ and $|B_1|$ are the absolute values of the amplitudes of A_1 and B_1 , and $*$ is the complex conjugate value. Using these values, the ratio (α) of the acoustic power dissipated in the orifice ($PW_{21tot} - PW_{22tot}$) to the acoustic power incident on the orifice (PW_{1inc}) is as follows:

$$\alpha = \frac{PW_{21tot} - PW_{22tot}}{PW_{1inc}} \quad (7)$$

In this paper where the end of Field 3 is a complete reflection, since PW_{22tot} is 0, the above equation is PW_{21tot}/PW_{1inc} , which is equivalent to the definition of sound absorption coefficient. Therefore, in this paper, the ratio of the acoustic power consumed inside the orifice to the acoustic power incident on the orifice was evaluated by the sound absorption coefficient (α).

B. Experimental Equipment and Sound Absorption Rate

Figure 3 shows a schematic diagram of the experimental apparatus. Field 1 and Field 3 are squares with a cross section of 200 mm \times 200 mm, and the lengths of Field 1 and Field 3 in the longitudinal direction are 500 mm and 334 mm, respectively. The duct is made of acrylic plates whose thickness is 5mm. The perforated plates are shown in Figure 4, the radius of the orifice, the length of the orifice and the aperture ratio are the parameters. A sine wave generated by a PC was amplified by an amplifier, and a sound was transmitted from a speaker installed at the end of the duct. Four microphones were suspended from the top of the duct to a position 50 mm, and the sound pressure was measured. The four microphones are Mic.1 to Mic.4, Mic.1 is 170 mm from the perforated plate surface to the speaker side, Mic.2 is 120 mm, Mic.3 is 65 mm downstream from the perforated plate

surface, Mic. 4 was installed at 115 mm. The measured sound pressure was converted to frequency data using an FFT analyzer, and the sound pressure amplitude from Mic.1 to Mic.4 and the relative phase angle with respect to Mic.4 were obtained from Mic.1 to Mic.3. These series of operations are carried out using a PULSE analyzer manufactured by Brüel & Kjær. The various settings are measurement frequency range: 0 to 1000 Hz, frequency interval: 1.25 Hz, overlap rate: 50%, The sweep speed of the sine wave was 1.6 Hz / s. The actual sound absorption coefficient calculation method is as follows. First, the complex sound pressure P_{Micm} (m is the number of the microphone) and the coordinate value of the microphone are input to Equations (1) and (2) to obtain A_1 , B_1 , A_3 , and B_3 . Then, using these values and the coordinates of the perforated plate surface, $p_1|_{x=x_1}$, $v_1|_{x=x_1}$, $p_2|_{x=x_2}$ and $v_2|_{x=x_2}$ is obtained, and various sound power values are obtained using Equations (3) to (6).

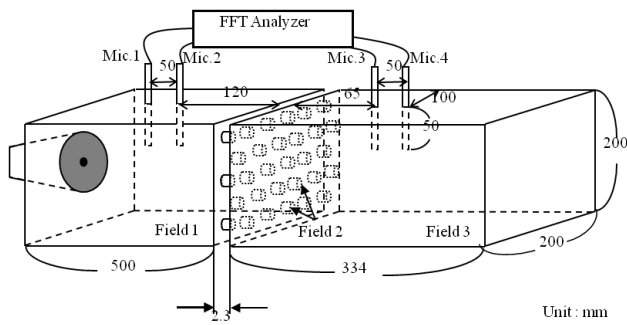


Figure 3. Experimental Setup.

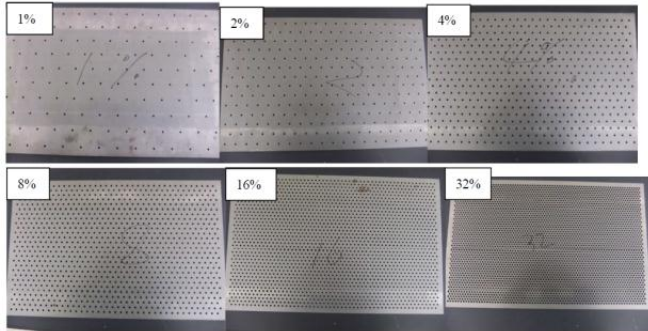


Figure 4. Perforated plates with several aperture ratios.

C. Numerical Analysis Model and Calculation Method of Sound Absorption Rate by Numerical Analysis

Applying Equations (1) and (2) to Field 1 and Field 3, the following equations are obtained.

$$p_1 = j\omega\rho_1(A_1\exp[-jk_1x] + B_1\exp[jk_1x]) \quad (8)$$

$$v_1 = jk_1(A_1\exp[-jk_1x] - B_1\exp[jk_1x]) \quad (9)$$

$$p_3 = j\omega\rho_3(A_3\exp[-jk_3x] + B_3\exp[jk_3x]) \quad (10)$$

$$v_3 = jk_3(A_3\exp[-jk_3x] - B_3\exp[jk_3x]) \quad (11)$$

Also, the sound pressure ($p_1|_{x=x_1}$) and acoustic particle velocity ($v_1|_{x=x_1}$) at the connection between Field1 and Field2, the sound pressure at the connection between Field2 and Field3 ($p_3|_{x=x_2}$), and the acoustic particle velocity ($v_3|_{x=x_2}$) can be expressed as

$$\begin{pmatrix} p_1|_{x=x_1} \\ v_1|_{x=x_1} \end{pmatrix} = \begin{bmatrix} 1 & \Gamma \\ 0 & 1 \end{bmatrix} \begin{pmatrix} p_3|_{x=x_2} \\ v_3|_{x=x_2} \end{pmatrix} \quad (12)$$

Here, Γ is the acoustic impedance. In this paper, we compared the case of using the simple equation and the case of using Melling equation. Since the acoustic particle velocity is V_0 at the sound wave transmission position ($x=0$) at the left end of the tube, the acoustic particle velocity is 0 at the other tube end ($x=x_3$), and Field1 and Field3, they are connected by equation (12), the boundary conditions are expressed as follows.

$$v_1|_{x=0} = V_0 \quad (13)$$

$$v_3|_{x=x_3} = 0 \quad (14)$$

$$p_1|_{x=x_1} = p_3|_{x=x_2} + \Gamma \cdot v_3|_{x=x_2} \quad (15)$$

$$v_1|_{x=x_1} = v_3|_{x=x_2} \quad (16)$$

$$Z = p_1|_{x=x_1} / v_1|_{x=x_1} \quad (17)$$

$$\alpha = 1 - \left(\frac{Z - \rho_1 c}{Z + \rho_1 c} \right)^2 \quad (18)$$

Four variables A_1 , A_3 , B_1 , and B_3 can be obtained by introducing the boundary conditions of equations (13) through (16) into equations (8) through (11). From these values, various sound power values can be obtained in the same way as in the actual measurement, or the sound absorption coefficient can be obtained by using equations (17) and (18). The case where the simple equation is used for Γ is referred to as "sound absorption coefficient using the simple equation" and the case where Melling equation is used for Γ is referred to as "sound absorption using Melling equation". The simple and Melling equations are shown in Sections II.D and E.

D. Acoustic Impedance Calculated by Simple Formula

The impedance Γ of the perforated plate is calculated as follows. The acoustic impedance of the hole considering the acoustic radiation at the end of the hole of the perforated plate and the acoustic energy due to the viscosity and heat exchange at the inner wall of the hole is expressed by the following equation.

$$\Gamma = R + j\rho\omega \frac{t_0 + 2\delta d}{\sigma} \quad (19)$$

Where t_0 : Orifice length, d : Orifice diameter, and σ : Opening ratio. R is the acoustic resistance that takes into account the acoustic energy dissipation due to viscosity and heat exchange at the inner wall of the hole, and $2\delta d$ is the open end correction on both sides of the hole. These parameters are expressed as the following empirical equations [6].

$$R = 4 \frac{R_v t_0 + t_m}{\sigma d} = 4R_v \frac{1+t_0/d}{\sigma} \quad (20)$$

$$\delta = 0.4(1 - 1.47\sigma^{0.5} + 0.47\sigma^{1.5}) \quad (21)$$

Where R_v : viscous resistance coefficient ($\cong 0.83 \times 10^{-2} \sqrt{f}$), t_m : additional resistance correction length ($\cong d$).

E. Acoustic Impedance Calculated by Melling formula

Melling theoretically investigated the acoustic power attenuation of sound waves in Field 2 with a small cross-sectional area by “viscosity and heat exchange of air particles” or “effect of flow ejected from the orifice acting on air outside orifice” is expressed as follows [4].

$$\text{Re}(\Gamma) = \frac{2(t_0+d)}{a} \sqrt{2\rho\mu\omega} \cdot a + \frac{8}{3\pi} \frac{1}{C_d^2} \{a^2 - 1\} \frac{\rho}{2} \hat{u} \quad (22)$$

$$\text{Im}(\Gamma) = \rho\omega \left\{ t_0 \left(1 + \frac{2}{d} \sqrt{\frac{2\mu}{\rho\omega}} \right) + \frac{8}{3\pi} d \right\} a \quad (23)$$

Where $1/a$: aperture ratio, μ : viscosity coefficient, C_d : flow coefficient, \hat{u} : effective value of acoustic particle velocity at the orifice. In this paper, μ is 1.882×10^{-5} Pa.s, and C_d is 0.63 from Melling measurements [4].

III. NATURAL FREQUENCY OF EACH PART

In this chapter, the natural frequency of each part was examined as a preliminary preparation for considering the measurement results and analysis results.

A. Natural Frequency of Each Part

The Helmholtz resonator model shown in Fig. 5 is generally used to study the sound absorption mechanism of a perforated plate.

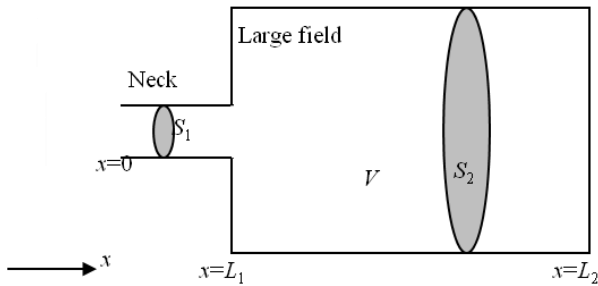


Figure 5. Schematic Diagram of Connected System of Neck Part and Large Field Part

This model is the one-degree-of-freedom system composed of a neck corresponding to the orifice and a large space connected to it, and its resonance frequency is given by the following equation.

$$f = \frac{c}{2\pi} \sqrt{\frac{S_1}{VL_1}} \quad (24)$$

Where S_1 is the cross-sectional area of the neck part, L_1 : the length of the neck part, and V is the volume of the large field part.

On the other hand, this paper includes a frequency range that cannot be expressed by the one-degree-of-freedom system. In addition, within the aperture ratio applied in this paper, there is a case where “volume of neck portion \ll volume of large field part” assumed by Equation (24) is not satisfied. Therefore, in this paper, to obtain the resonant frequency of the Helmholtz resonator, we used the Equation (33) obtained by applying the one-dimensional Helmholtz equation to the neck and large field instead of Equation (24). The derivation process of Equation (33) is as follows. Equations (1) and (2) are applied to both fields with the neck as Field 1 and the large field as Field 2.

$$p_1 = j\omega\rho_1(A_1 \exp[-jk_1x] + B_1 \exp[jk_1x]) \quad (25)$$

$$v_1 = jk_1(A_1 \exp[-jk_1x] - B_1 \exp[jk_1x]) \quad (26)$$

$$p_2 = j\omega\rho_2(A_2 \exp[-jk_2x] + B_2 \exp[jk_2x]) \quad (27)$$

$$v_2 = jk_2(A_2 \exp[-jk_2x] - B_2 \exp[jk_2x]) \quad (28)$$

The sound pressure is 0 at the neck opening ($x=0$), and the acoustic particle velocity is V_0 ($V_0 = 0$) at the end of the large field ($x=L_2$). At the space connection, the sound pressure and the volume velocities of acoustic particles on the both sides of the neck and large field are equal.

$$p_1|_{x=0} = 0 \quad (29)$$

$$v_2|_{x=L_2} = V_0 = 0 \quad (30)$$

$$p_1|_{x=L_1} = p_2|_{x=L_1} \quad (31)$$

$$v_1|_{x=L_1} S_1 = v_2|_{x=L_1} S_2 \quad (32)$$

By introducing the boundary conditions of Equation (29) to Equation (32) into Equation (25) to Equation (28), we can obtain four variables A_1 , A_2 , B_1 , and B_2 , and obtain response values in space. The denominators of variables A_1 , A_2 , B_1 , and B_2 are common, and the frequency at which these become 0 is the resonance frequency. If the denominators are set to 0, the equation (33) is obtained.

$$\left(\frac{1}{a} - 1\right) \cos\left(\frac{4L_1\pi f}{c} - \frac{2L_2\pi f}{c}\right) + \left(\frac{1}{a} + 1\right) \cos\left(\frac{2L_2\pi f}{c}\right) = 0 \quad (33)$$

Table 1 shows the first- and second-order spatial resonance frequencies at each aperture ratio when Field 2 in Fig. 2 is considered as the neck part and Field 3 is considered as the large field part. The aperture ratio $1/a$ is S_1/S_2 , where S_1 is the cross-sectional area of the neck and S_2 is the cross-sectional area of the large field. At $x=L_1$ which indicates the length of Field 2, the speed of sound was set to 347.4 m/s, taking account of the open end correction. As the aperture ratio increases, the resonance frequencies increase shown in Table 1.

TABLE I. FIRST AND SECOND RESONANCE FREQUENCIES

Aperture ratio [%]	1st resonance freq. [Hz]	2nd resonance freq. [Hz]
8	220.7	674.6
4	193.6	624.4
2	159.2	581.9
1	123.5	553.7
0.5	91.9	537.5

IV. EXPERIMENTAL AND NUMERICAL RESULTS

A. Comparison of measured and analyzed values in case without perforated plate

The frequency response of the sound pressure level was compared between the measured and the analytical values to confirm the consistency between the measured value and the numerical analysis model. Here, the model without the perforated plate was used, and the evaluation point was 565 mm from the sound source surface (Mic. 3). The purpose here is to compare the characteristics of the frequency response diagram for the measured and the analytical values. Therefore, the work is not performed to match the acoustic particle velocity of the input vibration surface between the measured value and the analysis. 1 mm/s at 0 and 0.25 mm/s at 850 Hz, and other frequencies were given by linear interpolation from these values. Figure 6 shows the frequency response of the sound pressure level at the evaluation point.

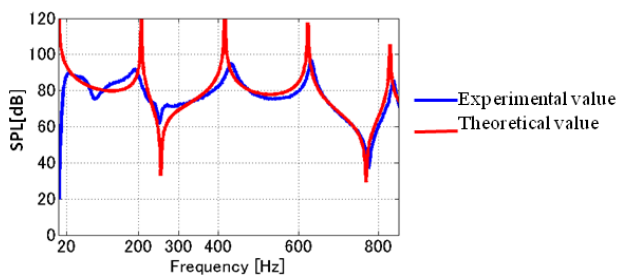


Figure 6. SPL at x=565 mm (Mic.3) measured and calculated theoretically.

Below 20 Hz, there is a large difference between the measured and analytical values. In the model with both ends closed, when approaching 0 Hz, the wave numbers k_1 and k_3 approach 0 and should diverge infinitely from Eqs. (8) to (17). This is the limit of the measurement, and in this paper, we decided to discuss the results above 20 Hz. There is one peak and one dip in the analytical value in the range of 20 Hz to 300 Hz. The peak and dip corresponding to the analytical values are also confirmed in the measured values, however the analytical and measured values are different. Furthermore, peaks and dips those are not represented in the analytical values were observed in the measured values. These were considered to be the phenomena caused by tube wall vibration, as described later. Above 300 Hz, there were three peaks and one dip, and it was confirmed that the measured values and the analytical values were almost the same. In addition, the sound pressure level in

the experimental apparatus used in this study is less than 100 dB, not the high sound pressure, as shown in Fig. 6, even at the peak value.

Next, the sound absorption without using a perforated plate was compared between measured and analyzed values. Figure 7 shows the sound absorption coefficient (α). The analytic value of the sound absorption coefficient is 0 because there is no perforated plate, however the measured value in the frequency range evaluated in the measurement is about 0.1. It is assumed that the sound is transmitted due to the elasticity of the tube wall or errors in the measurement. In any case, it was confirmed that the measured values include an error of about 0.1.

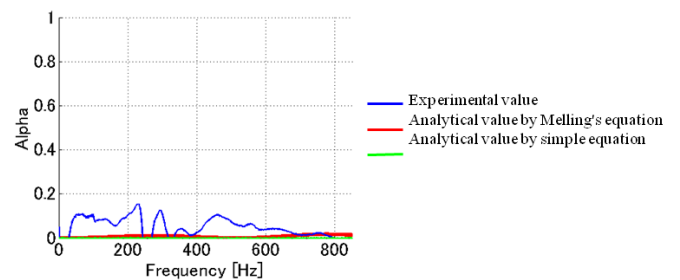


Figure 7. Absorbent coefficient measured and calculated theoretically in case without perforated plate.

B. Effect of aperture ratio on sound absorption coefficient

In order to investigate the effect of the aperture ratio on the sound absorption coefficient (α) and to confirm the usefulness of Melling and the simple equations, the sound absorption coefficient was calculated using each equation and compared with the measured sound absorption coefficient. Here, the orifice length was 2.3 mm, the orifice diameter was 3.0 mm, and the aperture ratios were 8%, 4%, 2%, 1%, 0.5%, and 0.0% (plates with no orifice open). The results are shown in Fig. 8. In addition, the symbols Pf1, Pf2, Ps1, Ps2, and Ps3 are given to the peaks that can be confirmed in the figure. Pf is a peak that is considered to be related to the medium and orifice, and Ps is a peak that is considered to be related to structural vibration. The numbers are assigned in order from the lowest frequency. In Fig. 8, the red (—) and green (—) lines represent the sound absorption rates using Melling equation and the simple equation, respectively. The blue line (—) represents the measured sound absorption rate.

As shown in Figs. 8 (a) to 8 (e), the peak value of the sound absorption coefficient increases as the aperture ratio decreases. It is considered that the smaller the aperture ratio is, the higher the particle velocity of the sound pressure passing through the hole becomes and the greater the damping due to friction becomes. In the case of the aperture ratio of 0.0% shown in Fig. 8 (f), there is a rigid body wall that has no orifice and the acoustic pressure is completely reflected in the tube. The sound absorption coefficient is theoretically 0.0. However, the measured sound absorption coefficient exceeded 0.4 at maximum in the frequency range below 400 Hz. The reason for this will be described later.

In Fig. 8 (b), in the case that the aperture ratio is 4%, Pf1 was not confirmed in the measurement, however Pf1 was confirmed at other aperture ratios above 0.5%. In Figs. 8 (d) and 8 (e) in cases that the aperture ratio is 1%, Pf1 indicated by the two analytical values those are calculated by the simple and Melling equations and the measured value Pf1 corresponding with the two analytical values were confirmed. As the aperture ratio decreases, the peak frequency of Pf1 decreases, the peak value increases, and the half-value width decreases in both the analysis and measurement. Furthermore, Pf1 cannot be confirmed in Fig. 8 (f) with an aperture ratio of 0%. The frequency of Pf1 in Figs. 8 (d) and 8 (e) is 124 Hz and 91 Hz in the measured values, and they correspond well with resonance frequencies of 124 Hz and 92 Hz. Therefore, Pf1 is assumed to be the resonance frequency associated with Field 2 and Field 3. In Fig.8 (f), since the aperture ratio is 0%, it is considered that Pf1 due to the acoustic phenomenon related to Field 2 and Field 3 does not occur.

Pf2 was observed in Fig. 8 (a) to (e). However, as can be seen from Figs. 8 (d) and 8 (e), when the aperture ratio is below 1%, the half-value width of Pf2 is narrow, therefore accurate sound absorption coefficient cannot be measured, and the peak value of the analytical value does not agree with the measured one. As the aperture ratio decreases, the peak frequency decreases, and the peak value increases, and the half-value width decreases. These tendencies were confirmed by both analytical values and measured values. The measured values of Pf2 in Figs. 8 (a) to 8 (e) are 701 Hz, 641 Hz, 606 Hz, 570 Hz, and 553 Hz, respectively. The analytical values of the secondary resonance frequencies in Table 1, agrees with the measured values with a few percent error. These results show that Pf2 is the secondary resonance frequency of Field 2 and Field 3.

There is no difference between the sound absorption coefficient calculated using Melling equation and that calculated using the simple equation except the peak value on the low frequency side. Regarding the peak value on the low frequency side, the sound absorption coefficient calculated using Melling equation was closer to the measured value than that calculated using the simple equation.

Next, with respect to the structural transmitted sound on the wall of the tube, the same phenomenon is assumed to occur at the aperture ratio of 0% and the aperture ratio of 0.5%. The analytical value of the sound absorption coefficient was modified by adding the measured value at 0% to the analytical value obtained using Melling equation at 0.5%. The analytical value at 0.5% in Fig. 8(f) is the value calculated by taking only the acoustic phenomenon of the perforated plate part into consideration, and the measured value at 0% is regarded as the one including the structure-acoustic phenomenon other than the perforated plate part. The modified value, which is the sum of the two, can be considered to be equivalent to the measured value at 0.5%. The results are shown in Fig. 9. Since the modified and the measured values are in good agreement, the same phenomenon as the transmitted sound that occurs when the aperture ratio is 0% seems to occur when the aperture ratio is 0.5%.

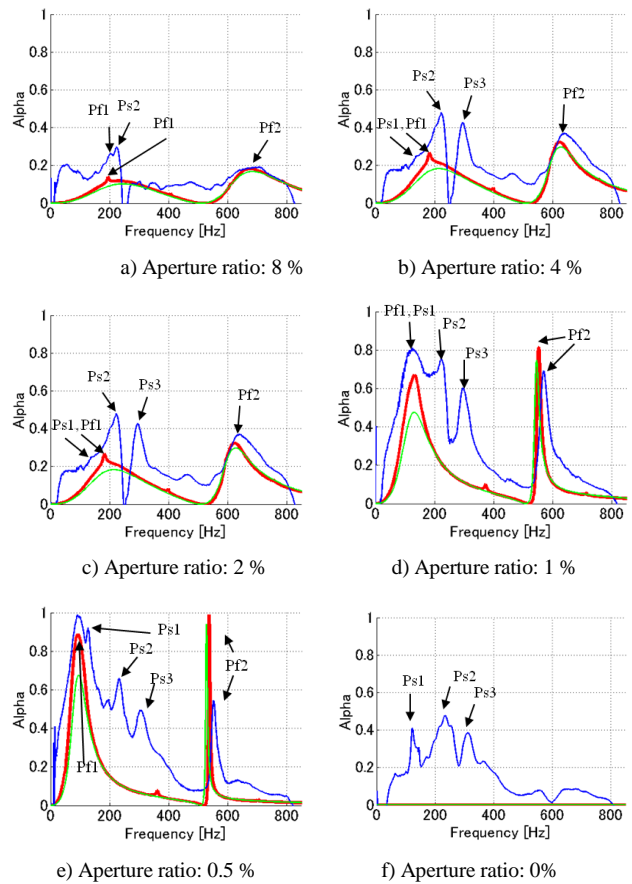


Figure 8. Frequency response of absorbent values of various aperture ratios. (Orifice diameter: 3.0 mm, Orifice length : 2.3 mm)

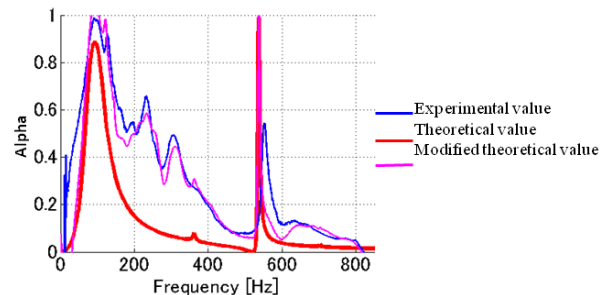


Figure 9. Absorbent values measured and calculated theoretically using modifying by summation of absorbent coefficients in the cases of the aperture ratio 0% and 0.5% (Orifice diameter : 3.0 mm, Orifice length : 2.3 mm)

Finally, Fig. 10 shows the measured values of the sound pressure on the upstream surface of the perforated plate at 8% and 0%, and the analytical value using Melling equation. The measured value does not exceed 100 dB over the entire frequency range, however the analytical value using Melling equation shows the good agreement with the measured value. Therefore Melling equation seems to be applicable even in case that the sound pressure is below 100 dB.

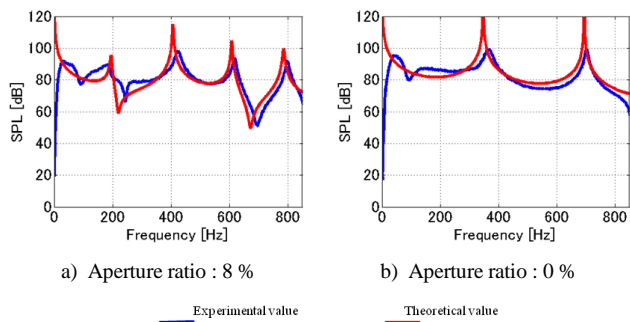


Figure 10. SPL at the upstream side of the plate.

Summarizing the above, the sound absorption rate increases at the acoustic resonance frequency of the system formed by Field 2 and Field 3. When the aperture ratio decreases, the peak frequency of the sound absorption coefficient and the half width decreases and the peak value increases. These results were confirmed by both the measured and analytical values. It was also confirmed that Melling equation was applicable even at sound pressure levels below 100 dB. The comparison between the simple and Melling equations shows that the peak frequency of the sound absorption coefficient agrees well, however the peak value calculated by Melling equation is closer to the measured value than that calculated by the simple equation.

C. Effect of natural frequency of structural vibration on sound absorption coefficient

Since the sound leakage due to vibration of the acrylic wall of the tube is assumed to affect the sound absorption coefficient, the natural frequency of the acrylic tube at below 500 Hz was obtained using the commercial finite element method code ANSYS 18.0. Figure 11 shows the structural model used in the modal analysis. The acrylic structural properties are Young's modulus of 3140 MPa, density of 1190 kg/m³ and Poisson's ratio of 0.35. Shell type elements were used for modeling, and one element length was about 1 cm.

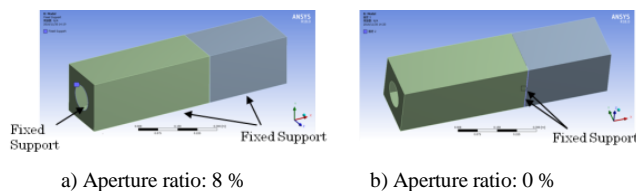


Figure 11. Boundary conditions in the modal analysis.

In the case of the aperture ratio of 0.0% shown in Fig. 8 (f), the tube has no orifice and rigid body walls that completely reflects the sound in the numerical model. Therefore, the sound absorption coefficient is theoretically 0.0. However, the measured sound absorption coefficient exceeded 0.4 at maximum in the frequency range below 400 Hz. The structural modes are shown in Table 2. The peak frequencies of Ps1, Ps2, and Ps3 observed in Fig. 8 (f) are 122 to 138 Hz for Ps1, 221 to 240 Hz for Ps2, and 278 to 311 Hz for Ps3, respectively. Ps1 is excited by the first order (126.4 Hz) of ID1 in Table 2, and the peaks of Ps2 and Ps3 are generated by excitation of the structural modes of ID3 (238.96 Hz) and ID1 (282.17 Hz) in Table 2. Therefore, the sound power of Field 1 is assumed to leak to the external space due to these structural modes. The leaked sound power is evaluated as PW_{21tot} in Equation (7), and the sound absorption coefficient shows a large value. It can be considered that the sound absorption coefficient at the aperture ratio of 0.0% is above 0 and generated by the structural vibration. In addition, in Figs. 8 (a) to 8 (e), the sound absorption generated by the structural vibration is observed at almost the same frequency (although the case that Ps1 is not observed exists). Below 500 Hz, the measured sound absorption coefficient is larger than the calculated sound absorption coefficient without taking account of the structural vibration. It was found that the sound absorption coefficient of the perforated plate was affected by the structural modes of the tube.

D. Effect of orifice length on sound absorption

In order to investigate the effect of orifice length on sound absorption, the following experiment was performed. The orifice diameter and the aperture ratio are fixed at 3.0 mm and 1%, respectively and the orifice lengths are 1.0 mm, 2.3 mm, and 4.6 mm. Figure 12 (b) shows the same data as Figure 8 (d). As the orifice length increases, it was confirmed that the peak frequency decreases, the peak value increases, and the half-value width decreases in the analytical values of Pf1 and Pf2. The measured values showed the same tendency as the analytical values for the decrease in the peak frequency and the half width of Pf1 and Pf2. However, the increase in the peak value cannot be confirmed for both Pf1 and Pf2. The peak value of Pf1 shows a slight change in the sound absorption coefficient, as indicated by the analytical values, and is around 0.7 in all cases. Therefore, the increase of the peak value is not captured in the measurements. As can be seen from the analytical values, the peak value at Pf2 has the narrow half-value width of Pf2, and it is assumed that the sound absorption coefficient has not been measured accurately. This is the reason why the phenomenon of the increase in the peak value was not captured. The peak frequencies of Ps2 and Ps3 do not change, however the peak values change. The changes in the peak values of Ps2 and Ps3 are likely due to the change in the value of the Pf1 width.

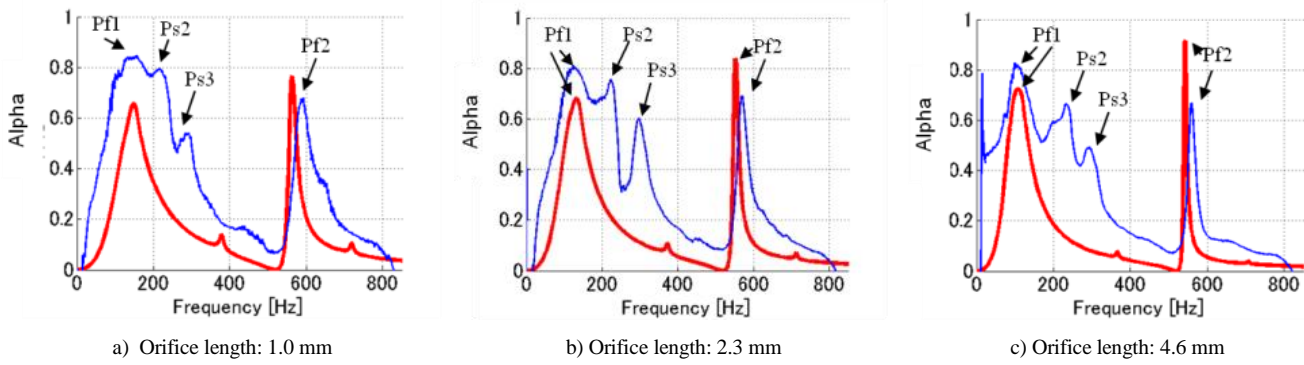


Figure 12. Frequency response of absorbent coefficients in cases of various orifice lengths. (Aperture ratio: 1 %, Orifice diameter : 3.0 mm)

E. Effect of orifice diameter on sound absorption

In order to investigate the effect of orifice diameter on sound absorption, the following experiment was performed. The orifice length and the aperture ratio are fixed at 1.0 mm and 1%, respectively and the orifice diameters are 3.0 mm, 2.0 mm and 1.0 mm.

As the orifice diameter decreases, the peak values of Pf1 and Pf2 increases and the half-value width increases as shown in Figure 13. The peak frequency of Pf1 and Pf2 increases slightly. In the measured values, the same phenomenon is confirmed in both Pf1 and Pf2.

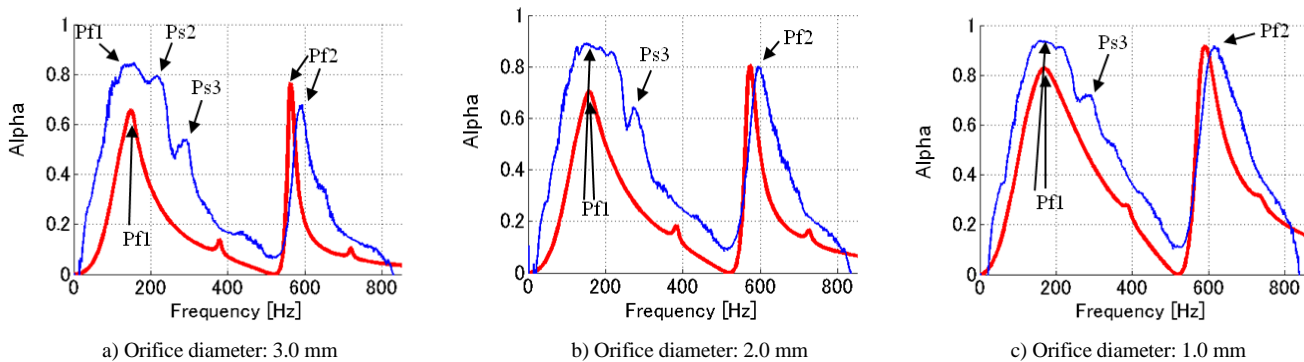


Figure 13. Frequency response of the absorbent values in cases of the various orifice diameter. (Aperture ratio: 1 %, Orifice diameter : 3.0 mm)

V. CONCLUSION

In this paper, under normal sound pressure (less than 100 dB), for several types of perforated plates with an aperture ratio of 0.5% to 8%, orifice length of 1.0 mm to 4.6 mm, and orifice diameter of 1.0 mm to 3.0 mm, we compared the sound absorption rate by calculating using the simple and Melling equations with the measured sound absorption rate, and obtained the following conclusions.

- The measurements and analysis show that the peak frequency moves to a lower frequency, the half-value width narrows, and the peak value increases as the aperture ratio decreases. In other words, the sound absorption coefficient increases as the aperture ratio decreases. The measurements and analysis show that the peak frequency shifts to a lower frequency and the half-value width becomes narrower as the orifice length is extended. As the orifice diameter decreases, the analytical value and the measured value show that the peak

frequency does not change, and the half width and peak value increases.

- The structural mode of the tube has a large effect on the sound absorption coefficient, especially at low frequencies below 500 Hz. In particular, below 500 Hz, the sound absorption coefficient obtained by actual measurement is larger than the sound absorption coefficient predicted by the simple and Melling equations that do not take structural vibration into account. There is the large difference between the measured and predicted values of the sound absorption coefficient.

- The sound absorption rates calculated using Melling and the simple equations show the agreement with the measured values in terms of the characteristics of the change in the sound absorption rate with respect to the change in the aperture ratio. However the peak value calculated using Melling equation is higher than that using the simple equation. The sound absorption rate calculated using Melling equation is

closer to the measured data than that using the simple equation. It was confirmed that Melling equation is applicable to all perforated plates in this range even under normal sound pressure below 100 dB.

[5] H. Utsuno, T. Itaya, Experimental study of Sound Absorbing characteristics for perforated panel by Four-microphone measuring technique, Proceedings of JSME Dynamics and Design Conference, (647), 2001.
 [6] INCE-Japan edit., Noise Control Engineering Hand Book, Gihodo Shuppan , 2001.

REFERENCES

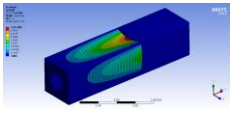
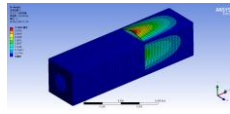
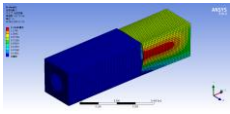
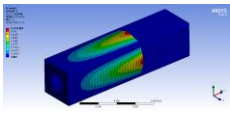
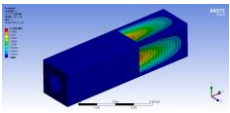
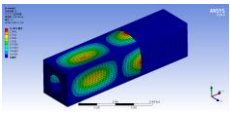
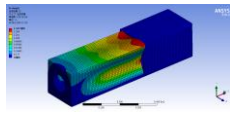
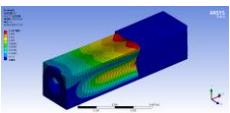
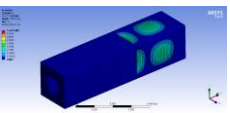
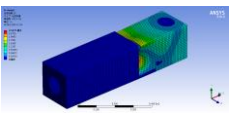
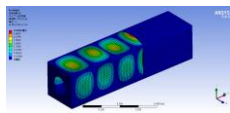
[1] R. C. Baird, Architectural Acoustics, CORONA PUBLISHING, 1988.
 [2] M. Koyasu, Fundamentals on Sound Absorption and Sound Absorbing Materials, Architectural acoustic and noise control, (71), 1990.
 [3] K. Ishihara, M. Nakaoka, M. Nishioka, Study on a countermeasure for high level sound generated from boiler tube bank duct using walls made of perforated plate (In case of aperture ratio being more than 1%), Transactions of the JSME, 82 (841), 2016.
 [4] T. H. Melling, The acoustic impedance of perforates at medium and high sound pressure levels, Journal of Sound and Vibration, 29 (1), 1973, p.1-65.

How to Cite this Article:



Mori, M., Masumoto, T. & Ishihara, K. (2019) Study on Applicability of Melling Equation and Conventional Equation for Sound Absorption Coefficient Prediction of Perforated Panel at Low Sound Pressure Field. International Journal of Science and Engineering Investigations (IJSEI), 8(95), 76-84. <http://www.ijsei.com/papers/ijsei-89519-11.pdf>

TABLE II. STRUCTURAL EIGEN FREQUENCIES AND MODE SHAPES OF THE ACRYLIC PLATE.

	ID1	ID2	ID3	ID4
Ps1	 126.4 Hz	 130.3 Hz	 137.73 Hz	
Ps2	 219.64 Hz	 221.3 Hz	 238.96 Hz	 239.03 Hz
Ps3	 282.17 Hz	 290.43 Hz	 293.4 Hz	 299.53 Hz